ILD-PHYS-PROC-2019-xxx

Search for Extra Scalars Produced in Association with Muon Pairs at the ILC

Yan Wang[◇*], **Jenny List**[◇], **Mikael Berggren**[◇]

[◇] *DESY, Notkestraße 85, 22607 Hamburg, Germany*

[*] *College of Physics and Electronic Information, Inner Mongolia Normal University, Hohhot 010022,China*

E-mail: yan.wang@desy.de

on behalf of the International Large Detector concept group

We study the search for an extra scalar S boson produced in association with the Z boson at the International Linear Collider (ILC). The study is performed at center-of-mass energy of 500 GeV based on the full simulation of the International Large Detector (ILD). In order to be as model-independent as possible, the analysis uses the recoil technique, in particular with the Z boson decaying into a pair of muons. As a result, exclusion cross-section limits are given in terms of a scale factor k with respect to the Standard Model Higgs-strahlung process cross section. These predicted results, covering all possible masses of the extra scalars at the 500 GeV ILC, can be interpreted independently of the decay modes of the S boson.

1. Introduction

The motivation of our study is to find a new scalar S boson in the SZZ coupling since one or more extra scalars are predicted in many new physics models. However, the properties of 125 GeV scalar measured at the LHC are very similar to the Standard Model (SM) Higgs boson [1]. As a result, the new scalar's couplings to the SM particles will be highly suppressed [2]. Furthermore, the LEP/LHC constraints on the extra scalars always rely on the model details. Thus, a more precise analysis without model-dependent assumptions to a scalar with the small coupling is preferred. Although the OPAL collaboration has searched for light scalars (less than 100 GeV) in a model-independent way at LEP, the results are limited by the low luminosity [3]. The International Linear Collider (ILC) is a proposed electron-positron linear collider, whose luminosity will be over a thousand times higher than that of LEP, which makes the recoil mass technique more powerful to find such extra scalars [4]. The ILC can reach higher center-of-mass energies, which will cover more searching regions for the extra scalar. A preliminary version of this analysis has been reported at LCWS2017 [5], LCWS2018 [6] and ICHEP2018 [7].

2. Event Generation and Detector Simulation

The signal is $e^+ + e^- \to S + Z$ production, where the Z boson decays to a pair of muons. The decay branching ratios of S are fixed as same as the 125 GeV Higgs boson, but no use would be made of this assumption. For SM background events, bremsstrahlung and initial state radiation (ISR) are explicitly considered. The event samples are generated with 100% left-handed and right-handed beam polarizations, using the Whizard 1.95 Monte Carlo (MC) event generator [9]. Then the samples are reweighted with beam polarizations of $\pm 80\%$ for the electron beam and $\pm 30\%$ for the positron beam.

Pythia is used for event hadronization [8]. Then, the events are simulated with two detector configurations, the so-called ILD_l5_o1_v02 option (which is IDR-L) and ILD_s5_o1_v02 option (which is IDR-S), which is performed under DD4HEP framework based on Geant4. The detail description of IDR-L and IDR-S can be found in the IDR[12]. The $\gamma\gamma \to$ low p_T hadrons and e^+e^- seeable pairs are generated based on the cross section model, and overlaid to all MC samples before the reconstruction. Then all the events are reconstructed using PandoraPFA algorithm in the Marlin framework to reconstruct individual final state particles, so-called Particle Flow Objects (PFOs). For the SM background, we use the samples generated in the context of the ILD Design Report [12], the fractions of integrated luminosity 4000 fb^{-1} are dedicated to $(-+,+-,++,--) = (40\%, 40\%, 10\%, 10\%)$. For the signal, a total of 48 signal benchmark points are chosen in the range of $10 \leq M_S \leq 410$ GeV.

2.1 Event selection and Background Rejection

ILCSoft with the version of v02-00-02 is used for all the analysis [10]. Firstly, we use updated version of IsolatedLeptonTagging, with $E_{CAL}/p < 0.5$, $p > 10$ GeV, MVA cut > 0.8. The E_{CAL} is the energy deposit in the calorimeter system, and p is the track momentum. A multivariate double cone method is used for muon isolation identification in this processor. With this processor, we require the event to have at least one μ^+ and one μ^- for further analysis.

Then, a pair of oppositely charged muons is selected by minimizing the following χ^2 function:

$$\chi^2(M_{\mu^+\mu^-}, M_{\texttt{rec}}) = \frac{(M_{\mu^+\mu^-} - M_Z)^2}{\sigma^2_{M_{\mu^+\mu^-}}} + \frac{(M_{\texttt{rec}} - M_S)^2}{\sigma^2_{M_{\texttt{rec}}}}, \tag{2.1}$$

where $M_{\mu^+\mu^-}$ is the invariant mass of the muon pair, and $M_{\texttt{rec}}$ is the recoil mass, which is defined as:

$$M^2_{\texttt{rec}} = (\sqrt{s} - E_{\mu^+\mu^-})^2 - |\vec{p}_{\mu^+\mu^-}|^2. \tag{2.2}$$

$\sigma_{M_{\mu^+\mu^-}}$ and $\sigma_{M_{\texttt{rec}}}$ are detector resolutions of $M_{\mu^+\mu^-}$ and $M_{\texttt{rec}}$, which is calculated event-by-event from covariance matrix of 4-momentum. A very loose preselection is used for choosing the muon pair: $M_{\mu^+\mu^-} \in [M_Z - 40, M_Z + 40]$ GeV, $M_{rec} \in [0, 500]$ GeV. After selecting the muon pair, the bremsstrahlung and final state radiation photons from the muons are combined with the muons.

Figures 1 shows the invariant mass distribution after preselection, reconstruction uncertanty ($M^{PFO} - M^{MC}$) distribution, and detector resolution $\sigma_{M_{\mu^+\mu^-}}$ distribution of $\mu^+\mu^-$ pair for two fermion backgrounds and the $M_S = 20$ GeV signal process for IDR-L and IDR-S.

Similarly, we use ISRPhotonTagging to select isolated ISR photons. A multivariate double cone method is also used for photon isolation identification, with the MVA cut > 0.8. Figures 2 shows the isolated ISR photon tagging efficiency to the signal and background.

Background events are reduced by firstly considering kinematic variables only relying on muons (and the reconstructed Z boson): the invariant mass and transverse momentum of the muon pair, as well as the polar angle of the missing momentum.

The multivariate analysis is used to improve sensitivity. A gradient boosted decision tree technique (BDTG) is used which is implemented in TMVA [13] in ROOT. Two BDTGs are used. The first BDTG is trained for two fermion backgrounds. The second BDTG is trained for the four fermion backgrounds and other backgrounds. They are trained using the same 6 input variables: muon pair invariant mass, the polar angle of each muon, the polar angle of the muon pair, the opening angle of the muon pair, and the $\pi - (\phi_{\mu^+} - \phi_{\mu^-})$, where $\phi_{\mu^\pm}$ are the azimuthal angles of the muons with respect to the beam line. If an ISR photon is tagged, the two muons are boosted to the effective center-of-mass reference frame opposite of the ISR photon. These BDTG networks are trained with those variables in the effective center-of-mass reference frame.

Then, taking into account the ISR photon return effects, the two fermion background can be further rejected by ISR energy veto cuts. With these cuts, no information on the decay of S is needed, thus the expected results will be model-independent. A simplified cut table is shown in Table 1, where the cut values are choosed by optimizing significance.

The recoil mass distributions after these cuts are shown in Figure 3. Finally, the recoil mass cut is applied, which is very useful when $M_S > M_Z$. The event numbers after cuts for IDR-L and IDR-S, when $M_S = 20$ GeV, $M_S = 200$ GeV and $M_S = 400$ GeV, are summarized in Table 2 as an example, where the polarization is $(-,+)$ and the luminosity is 4000 fb^{-1}. The significance is defined as $S/\sqrt{S+B}$, where B is the background event number, and S is the signal event number and $S = k \times \sigma_{H_{SM}\mu\mu}(m_{H_{SM}} = m_S) \times \int Ldt$, where H_{SM} is the SM Higgs boson and $k = 1$ in Table 2.

3. Results

A likelihood analysis is applied for calculating 2 σ expected exclusion limits on k with a bin-by-bin comparison between the signal and background recoil mass histograms for each benchmark

(a) 2f invariant mass distribution

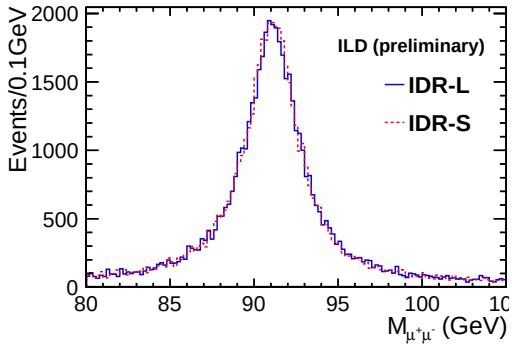

(d) $M_S = 20$ GeV signal invariant mass

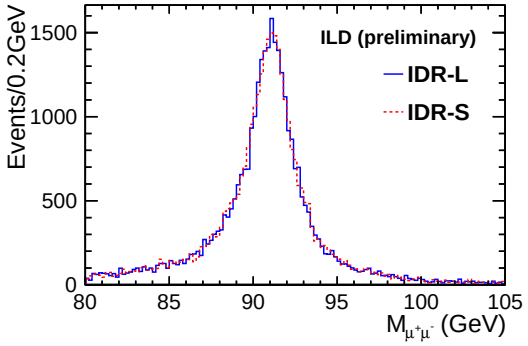

(b) 2f M_{PFO}-M_{MC}

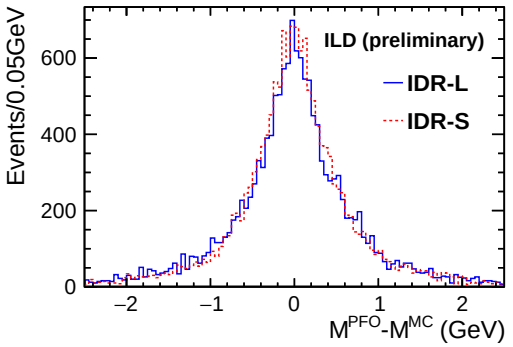

(e) $M_S = 20$ GeV signal M_{PFO}-M_{MC}

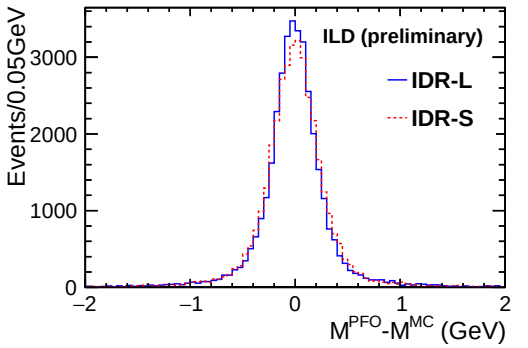

(c) 2f detector resolution $\sigma_{M_{\mu\mu}}$

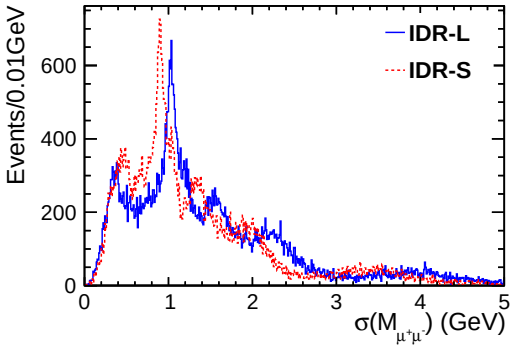

(f) $M_S = 20$ GeV signal resolution $\sigma_{M_{\mu\mu}}$

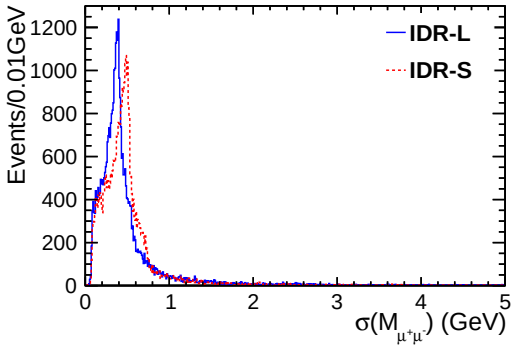

Figure 1: The muon pair invariant mass distribution, the muon pair invariant mass reconstruction uncertanty ($M^{PFO} - M^{MC}$) distribution, and the muon pair invariant mass detector resolution $\sigma_{M_{\mu\mu}}$ distribution for two fermion backgrounds and the $M_S = 20$ GeV signal process for IDR-L and IDR-S.

points and k_{95} is the 2 σ exclusion limits for the cross section scale factor k hereinafter. The signal-plus-background hypothesis and the background only hypothesis, which assumes that there is (not) a new higgs produced in the investigated mass range, are provided. Then a global test-statistic $Q(M_S) = L_{s+b}(M_S)/L_b(0)$ is constructed to discriminate signal and background, where $L_{s+b}(L_b)$ is the likelihood function for the signal plus background (only background) hypothesis. The normalized probability density function $Q(M_S)$ is integrated to provide the confidence levels $CL_b(M_S)$ and $CL_{s+b}(M_S)$. The ratio $CL_s(M_S) = CL_{s+b}(M_S)/CL_b(M_S)$ is used as the final confidence

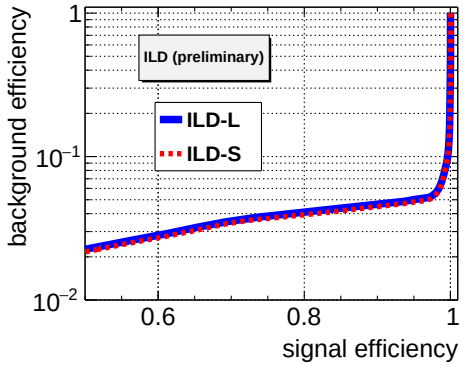

Figure 2: The isolated ISR photon tagging efficiency to the signal and background in IDR-L and IDR-S.

$M_{\mu^+\mu^-}$	$\in [70,110]$GeV
$P_T^{\mu^+\mu^-}$	$\in [0,245]$ GeV
$\sigma(M_{mu^+mu^-})$	$\in [0,1]$ GeV
MVA_{2f}	$[0.75,1]$
MVA_{4f}	$[0.5,1]$
ISR photon veto	$E_\gamma^{central} < 230$ GeV & $E_\gamma^{forward} < 150$ GeV
M_{rec}	$\in [M_S - 20, 450] GeV$

Table 1: The cut values after preselection in this analysis.

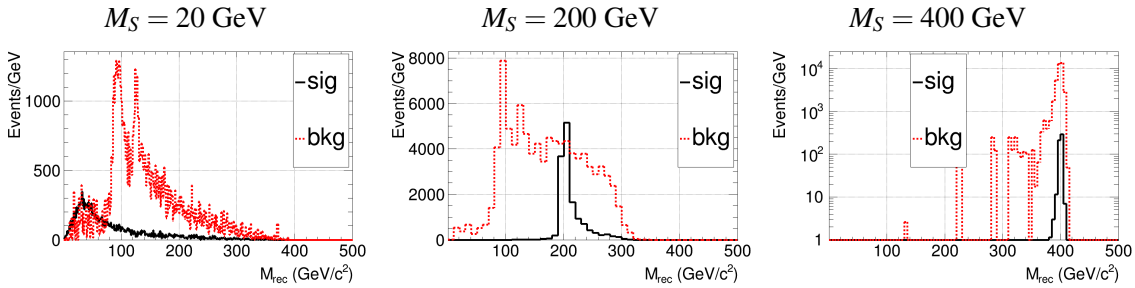

Figure 3: The recoil mass distributions after the ISR photon veto cut for signal and backgrounds, when $M_S = 20, 200, 400$ GeV and within IDR-L model.

level.

In Figure 4, a comparison of 2 σ exclusion limits between IDR-L and IDR-S is shown. The blue and red lines are the results for IDR-L and IDR-S. When $M_S < 340$ GeV, k_{95} is in the order of 10^{-1}, which could set strong model-independent constraints for the extra scalars. There are also OPAL's 2 σ exclusion limits, which are about one or two order weaker than ILC results.

In Figure 5, we compare the exclusion limits for the different final state levels when using IDR-L model. The black dashed line uses pythia stable particles, which only preserve pythia generator level information after hadronization. The blue line and red dashed line use IDR-L and IDR-S PFOs, respectively, which are well reconstructed with PFA. From this plot, we can see that in small mass region, there are still spaces for improvements.

(a) IDR-L, $M_S = 20$ GeV

	nh_{20}	h_{e2}	$4f_l$	$4f_{sl}$	$2f_l$	$6f_{all}$	*total bkg*	efficiency	significance
$M_{\mu^+\mu^-}$ & $P_T^{\mu^+\mu^-}$	18499	12013	253268	141395	1.3×10^6	14156	1.8×10^6	1	13.84
$\sigma(M_{mu^+mu^-})$	17111	11741	211576	115504	617247	13764	969833	0.92	17.22
MVA_{2f}	12168	10783	65416	63439	30815	6443.9	176896	0.66	27.98
MVA_{4f}	7289	5868.1	9033.3	14243.7	8710.1	444.8	38300	0.39	34.14
ISR photon veto	7283.4	5868.1	9032.7	14243.7	2722.2	444.8	32312	0.39	36.60
M_{rec}	7283.4	5868.1	9032.7	14243.7	2722.2	444.8	32312	0.39	36.60

(b) IDR-S, $M_S = 20$ GeV

	nh_{20}	h_{e2}	$4f_l$	$4f_{sl}$	$2f_l$	$6f$	*total bkg*	efficiency	significance
$M_{\mu^+\mu^-}$ & $P_T^{\mu^+\mu^-}$	18486	12011	257097	142154	1.4×10^6	15375	1.8×10^6	1	13.79
$\sigma(M_{mu^+mu^-})$	17380	11803	223684	120567	762838	15066	1.1×10^6	0.94	16.20
MVA_{2f}	12020	10752	66779	62017	33166	7138.5	179852	0.65	27.44
MVA_{4f}	7219.9	5840.8	9403.9	14321.9	9775.6	504.9	39847.1	0.39	33.28
ISR photon veto	7215.1	5838.2	9399.1	14322	2435.0	504.9	32499.1	0.39	36.21
M_{rec}	7215.1	5838.2	9399.1	14322	2435.0	504.9	32499	0.39	36.21

(c) IDR-L, $M_S = 200$ GeV

	nh_{200}	h_{e2}	$4f_l$	$4f_{sl}$	$2f_l$	$6f$	*total bkg*	efficiency	significance
$M_{\mu^+\mu^-}$ & $P_T^{\mu^+\mu^-}$	7021.0	10929	170024	128723	1.8×10^6	4901.4	2.1×10^6	1	4.81
$\sigma(M_{mu^+mu^-})$	6884.1	10657	119179	99931	569719	4507.8	803994	0.98	7.64
MVA_{2f}	6364.1	6862.1	32109	38841	14045	2537.7	94395	0.91	20.05
MVA_{4f}	5023.6	4649.6	11687	15146	5285.3	1090.2	37858	0.72	24.26
ISR photon veto	5023.6	4646.9	11668	15137	2324.4	1090.2	34866	0.72	25.15
M_{rec}	4972.4	1896.6	6643.0	4958.3	533.3	1058.5	15071	0.71	35.12

(d) IDR-S, $M_S = 200$ GeV

	nh_{200}	h_{e2}	$4f_l$	$4f_{sl}$	$2f_l$	$6f$	*total bkg*	efficiency	significance
$M_{\mu^+\mu^-}$ & $P_T^{\mu^+\mu^-}$	7083.1	11044	172482	130361	1.8×10^6	5097.2	2.1×10^6	1	4.83
$\sigma(M_{mu^+mu^-})$	6960.9	10833	129822	106170	807245	4788.0	1.1×10^6	0.98	6.74
MVA_{2f}	6428.2	7080.8	35365	40940	20011	2865.6	106262	0.91	19.15
MVA_{4f}	4907.9	4514.5	11537	15169	8291.9	1155.3	40668	0.69	22.99
ISR photon veto	4907.9	4514.5	11516	15169	2580.8	1155.3	34935.9	0.69	24.59
M_{rec}	4863.5	1875.1	6834.2	4949.9	915.7	1125.4	15700	0.69	33.92

(e) IDR-L, $M_S = 400$ GeV

	nh_{400}	h_{e2}	$4f_l$	$4f_{sl}$	$2f_l$	$6f$	*total bkg*	efficiency	significance
$M_{\mu^+\mu^-}$ & $P_T^{\mu^+\mu^-}$	237.3	502.0	125968	26464.9	1.0×10^6	6763.0	1.2×10^6	1	0.22
$\sigma(M_{mu^+mu^-})$	237.3	264.4	87410.1	4755.0	176159	6383.4	274972	1	0.45
MVA_{2f}	218.3	83.2	33981	1105.8	5945.6	3868.6	44984.1	0.92	1.03
MVA_{4f}	191.8	28.1	10757.1	707.0	4643.7	1289.3	17425.3	0.81	1.44
ISR photon veto	191.8	22.6	10657.2	687.8	1747.2	1289.0	14403.7	0.81	1.59
M_{rec}	191.4	19.9	10579.7	641.0	347.2	1279.6	12867.3	0.81	1.67

(f) IDR-S, $M_S = 400$ GeV

	nh_{400}	h_{e2}	$4f_l$	$4f_{sl}$	$2f_l$	$6f$	*total bkg*	efficiency	significance
$M_{\mu^+\mu^-}$ & $P_T^{\mu^+\mu^-}$	242.2	450.8	113163	19947.7	534691	7581.9	675835	1	0.29
$\sigma(M_{mu^+mu^-})$	242.2	276.0	86770	4743.7	115999	7280.3	215069	1	0.52
MVA_{2f}	219.2	93.7	32440.1	1266.9	5865.3	4622.5	44288.5	0.91	1.04
MVA_{4f}	188.7	35.8	11092.5	687.0	4769.9	1419.7	18005	0.78	1.40
ISR photon veto	188.7	33.0	11021.4	668.3	3264.2	1418.8	16405.6	0.78	1.46
M_{rec}	188.4	27.6	10973.9	649.6	2952.2	1414.9	16018.2	0.78	1.48

Table 2: The cut table of IDR-L and IDR-S, when $M_S = 20$, $M_S = 200$ and $M_S = 400$ GeVwhere the polarization is (-,+) and the luminosity is $\int Ldt = 4000 fb^{-1}$. The signal event numbers are supposed that $k = 1$.

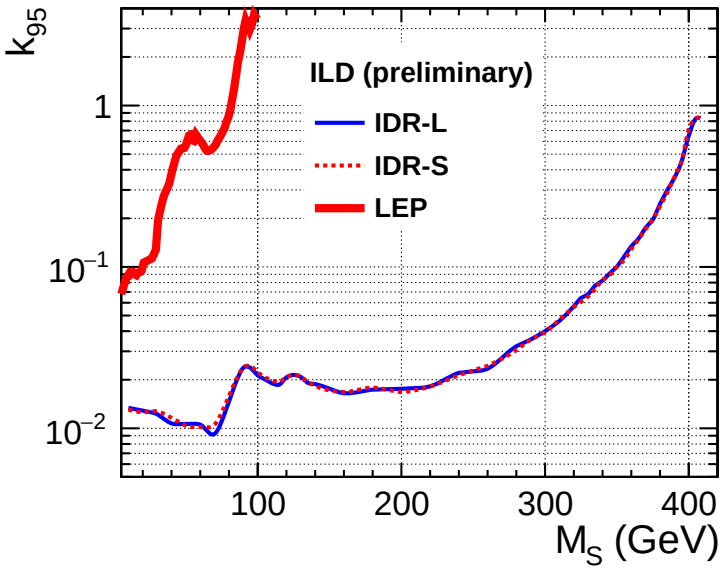

Figure 4: Preliminary Final Exclusion Limits for the cross section scale factor k for different scalar masses at 500 GeV ILC.

4. Conclusions

By applying the recoil technique, the potential of the ILC to search for scalars has been investigated at $\sqrt{s} = 500$ GeV center-of-mass energy, the fractions of integrated luminosity 4000 fb^{-1} are dedicated to $(-+,+-,++,--) = (40\%,40\%,10\%,10\%)$, with the full simulation of the ILD concept. The method is optimized to be independent of the scalar decay modes. 2 σ expected exclusion limits for the cross section scale factor k_{95} are shown for scalar mass from 10 GeV to 410 GeV when $\sqrt{s} = 500$ GeV. They are one or two orders of magnitudes more sensitive than those obtained at LEP, and covering substantial new phase spaces. No big difference between IDR-L and IDR-S is observed for this analysis.

Acknowledgements

We would like to thank the LCC generator working group and the ILD software working group for providing the simulation and reconstruction tools and producing the Monte Carlo samples used in this study. This work has benefited from computing services provided by the ILC Virtual Organization, supported by the national resource providers of the EGI Federation and the Open Science GRID. We are grateful for the support from Collaborative Research Center SFB676 of the Deutsche Forschungsgemeinschaft (DFG), Particles, Strings and the Early Universe, project B1. Y.W. is supported by the China Postdoctoral Science Foundation under Grant No. 2016M601134, and an International Postdoctoral Exchange Fellowship Program between the Office of the National Administrative Committee of Postdoctoral Researchers of China (ONACPR) and DESY.

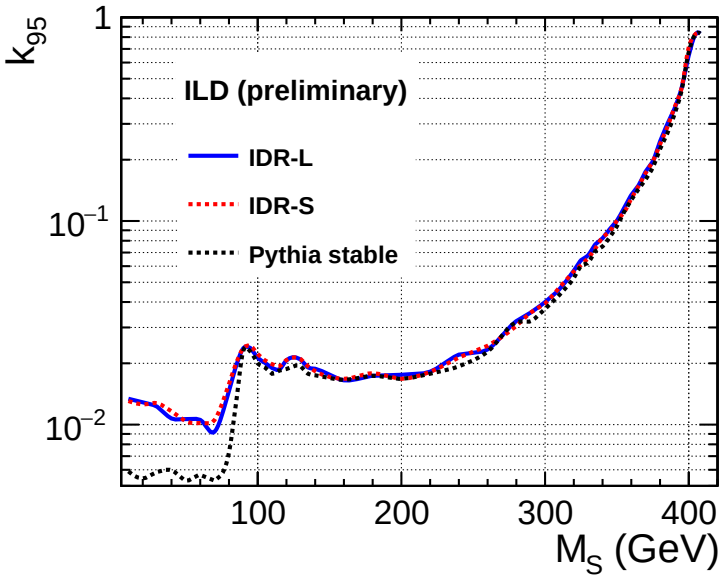

Figure 5: Exclusion Limits for the cross section scale factor k for different scalar masses, when comparing the reconstruction efficiency with pythia stable particles.

References

[1] The ATLAS and CMS collaboration, "Measurements of the Higgs boson production and decay rates and constraints on its couplings from a combined ATLAS and CMS analysis of the LHC pp collision data at $\sqrt{S} = 7$ and 8 TeV", JHEP 08 (2016) p.045.

[2] R. Aggleton et al., "Review of LHC experimental results on low mass bosons in multi Higgs models", JHEP 02 (2017) p. 035.

[3] G. Abbiendi , "Decay mode independent searches for new scalar bosons with the OPAL detector at LEP", Eur. Phys. J. C27 (2003) p. 311-329.

[4] D. M. Asner et al., "ILC Higgs White Paper", Proceedings, CSS2013 (2013) Minneapolis, USA, July 29-August 6, 2013.

[5] Y. Wang, J. List,and M. Berggren, "Search for Light Scalars Produced in Association with Muon Pairs for $\sqrt{s}$ = 250 GeV at the ILC", arXiv:1801.08164 [hep-ex].

[6] Y. Wang, J. List,and M. Berggren, "Search for Extra Scalars Produced in Association with Muon Pairs at the ILC", arXiv:1902.06118 [hep-ex].

[7] Y. Wang, J. List,and M. Berggren, "Search for Light Scalars Produced in Association with a Z boson at the 250 GeV stage of the ILC", ICHEP2018 Proceeding, PoS(ICHEP2018) 630.

[8] T. Sjostrand, S. Mrenna, and P. Z. Skands. PYTHIA 6.4 Physics and Manual. In: JHEP 05 (2006), p. 026. doi: 10.1088/1126-6708/2006/05/026. arXiv: hep-ph/0603175 [hep-ph].

[9] W. Kilian, T. Ohl and J. Reuter, "WHIZARD: Simulating Multi-Particle Processes at LHC and ILC", Eur. Phys. J. C **71**, 1742 (2011).

[10] ILCSOFT home page. In: (2017). url: http : / / ilcsoft . desy . de / portal

[11] H. Abramowicz et al., "The International Linear Collider Technical Design Report", ILC-REPORT-2013-040.

[12] ILD Detector Collaboration, "ILD Design Report" (2019).

[13] TMVA home page https://root.cern/tmva.

[14] R. Barate et al., "Search for the standard model Higgs boson at LEP", Phys. Lett. B565 (2003) p. 61-75.

[15] P. Drechsel, G. Moortgat-Pick, and G. Weiglein, "Sensitivity of the ILC to light Higgs masses", arXiv:1801.09662[hep-ph].